



1 **Measurement Report: Tropospheric and Stratospheric Ozone Profiles** 2 **during the 2019 TROPomi vaLIdation eXperiment (TROLIX-19)**

3
4 John T. Sullivan¹, Arnoud Apituley², Nora Mettig³, Karin Kreher⁴, K. Emma Knowland^{1,5}, Marc Allaart²,
5 Ankie Piters², Michel Van Roozendaal⁶, Pepijn Veeffkind², Jerry R. Ziemke^{1,5}, Natalya Kramarova¹, Mark
6 Weber³, Alexei Rozanov³, Laurence Twigg^{1,7}, Grant Sumnicht^{1,7}, and Thomas J. McGee^{1*}

7
8
9 ¹ NASA Goddard Space Flight Center, Greenbelt, MD 20771
10 ² Royal Netherlands Meteorological Institute (KNMI), De Bilt, Netherlands
11 ³ Institute of Environmental Physics, University of Bremen, Bremen, Germany
12 ⁴ BK Scientific GmbH, Mainz, Germany
13 ⁵ Morgan State University/GESTAR-II, Baltimore, MD 21251
14 ⁶ Belgian Institute for Space Aeronomie (BIRA), Ukkel, Belgium
15 ⁷ Science Systems and Applications Inc., Lanham, MD, 20706
16 *Now Emeritus

17 *Correspondence to:* John Sullivan (john.t.sullivan@nasa.gov)

18 **Abstract** A TROPospheric Monitoring Instrument (TROPOMI) validation campaign was held in the
19 Netherlands based at the CESAR (Cabauw Experimental Site for Atmospheric Research) Observatory
20 during September 2019. The TROPomi vaLIdation eXperiment (TROLIX-19) consisted of active and
21 passive remote sensing platforms in conjunction with several balloon-borne and surface chemical (e.g.
22 ozone and nitrogen dioxide) measurements. The goal of this joint NASA-KNMI geophysical validation
23 campaign was to make intensive observations in the TROPOMI domain in order to be able to establish
24 the quality of the L2 satellite data products under realistic conditions, such as non-idealized conditions
25 with varying cloud cover and a range of atmospheric conditions at a rural site. The research presented
26 here focuses on using ozone lidars from NASA's Goddard Space Flight Center to better evaluate the
27 characterization of ozone throughout TROLIX-19. Results of comparisons to the lidar systems with
28 balloon, space-borne, and ground-based passive measurements are shown. In addition, results are



29 compared to a global coupled chemistry meteorology model to illustrate the vertical variability and
30 columnar amounts of both tropospheric and stratospheric ozone during the campaign period.

31 **1 Introduction**

32 In September 2019, a joint Royal Netherlands Meteorological Institute (KNMI) and the U.S. National
33 Aeronautics and Space Administration (NASA) field campaign was performed in the Netherlands,
34 based at the Cabauw Experimental Site for Atmospheric Research (CESAR, 51.97° N, 4.93° E), to
35 provide the scientific community with additional information to further understand and evaluate the
36 Copernicus Sentinel-5 Precursor mission (S-5P) TROPOspheric Monitoring Instrument (TROPOMI)
37 instrument (<https://sentinels.copernicus.eu/web/sentinel/missions/sentinel-5p>). The main objective of
38 the Copernicus Sentinel-5P mission is to perform atmospheric measurements with high spatio-temporal
39 resolution, to be used for scientific studies and monitoring of air quality and chemical transport
40 (https://www.esa.int/Applications/Observing_the_Earth/Copernicus/Sentinel-5P).

41 To properly support satellite evaluation, the 2019 TROpomi vaLIIdation eXperiment (TROLIX-19)
42 campaign was designed to bring together many active and passive remote sensing platforms in
43 conjunction with several balloon-borne, airborne and surface measurements. Specifically, the
44 observations were established to provide geophysical verification in order to establish the quality of
45 TROPOMI Level 2 (L2) main data products under realistic non-idealized conditions with varying cloud
46 cover and a wide range of atmospheric conditions. Cabauw, using its comprehensive in-situ and remote
47 sensing observation program in and around the 213 m meteorological tower ([https://ruisdael-
48 observatory.nl/trolix19-tropomi-validation-experiment-2019/](https://ruisdael-observatory.nl/trolix19-tropomi-validation-experiment-2019/)) was the main site of the campaign with



49 focus on vertical profiling using lidar instruments for aerosols, clouds, water vapor, tropospheric and
50 stratospheric ozone, as well as balloon-borne sensors for nitrogen dioxide (NO₂) and ozone (Figure 1).
51 Although this work focuses primarily on the ozone lidar profiling during the study, the larger campaign
52 overview, background, and motivation can be found in Apituley *et al.* (2019; 2020) or Kreher *et al.*
53 (2020a).
54 One main goal of this work is also to understand ozone profile retrievals as they relate to upcoming
55 satellite endeavors. As NASA prepares to launch its first geostationary air quality satellite
56 “Tropospheric Emissions: Monitoring of Pollution” (TEMPO), this work also specifically establishes a
57 paradigm of evaluation for TEMPO-derived products such as tropospheric ozone columns and a 0-2km
58 tropospheric ozone product. Due to the finer spatial footprint, increased temporal frequency and vertical
59 extent of TEMPO’s tropospheric ozone retrievals, ozone lidars are an ideal platform to perform future
60 evaluations of the products, which builds from recent work done in Johnson *et al.*, 2018. Specifically,
61 this work will investigate the results from the combination of having a co-located NASA tropospheric
62 (Sullivan *et al.*, 2014) and stratospheric ozone lidars (McGee *et al.*, 1991) in order to obtain an entire
63 vertical profile of ozone from ~0.2km to 50km.
64 For the first time, this transportable combination of lidars is able to explicitly derive diurnally varying
65 tropospheric and total ozone columns, which are compared directly to measurements obtained by
66 ground-based passive sensors, current satellite instrumentation and chemical transport models. In
67 Section 2 we present all available data and methods used in this work, across the various platforms
68 during the TROLIX-19 study. Section 3 focuses on comparisons of the tropospheric ozone retrievals of
69 the vertical profiles of ozone within the troposphere and columnar reductions of 0-10 km and 0-2 km.



70 Comparisons of lidar data with available complete ozone profiles (Sec 4) and columnar amounts (Sec 5)
71 from several platforms and chemical transport models are also presented to further understand the
72 quality of satellite derived ozone profiles during the TROLIX-19 period.

73

74 2 Data and Methods

75 Descriptions of the various observational and model data sets and used in this study are below,
76 including a summary table (Table 1).

77 **2.1 NASA Ozone Differential Absorption Lidars (DIAL)**

78 NASA deployed and operated two ozone lidars during TROLIX-19 at the Cabauw site near the CESAR
79 tower to observe temporal and vertical gradients in tropospheric and stratospheric ozone. This was the
80 first dual-deployment of these lidars, in which the tropospheric ozone lidar measured between the near
81 surface (about 0.2 km) to a height of about 18 km and the stratospheric lidar during night-time from 15
82 km upwards to nearly 50 km, providing complete hybrid ozone profiles for the campaign period.

83 The NASA GSFC Mobile Stratospheric Ozone Lidar Trailer Experiment (STROZ-LITE) has been a
84 participant in the Network for the Detection of Atmospheric Composition Change (NDACC) since its
85 inception and is housed in a 12.5m container allowing for transport around the world (McGee et al.,
86 1991). The lidar instrument transmits two wavelengths, 308 nm from a XeCl excimer laser, and 355 nm
87 from a ND:YAG laser to derive ozone number density profiles, which have historically served as an
88 intercomparison data set for other NDACC ozone lidars (recent intercomparison can be found at Wing
89 *et al.*, 2020; 2021).



90 The NASA GSFC TROPOZ has been developed in a transportable 13.5m trailer to take routine
91 measurements of tropospheric ozone near the Baltimore–Washington, D.C. area as well as various
92 campaign locations (Sullivan *et al.*, 2014; 2015,2019, Leblanc *et al.*, 2018). This instrument, which
93 utilizes a ND:YAG laser and Raman cell, has been developed as part of the ground-based Tropospheric
94 Ozone Lidar NETwork (TOLNet, <https://www-air.larc.nasa.gov/missions/TOLNet/>), which currently
95 consists stations across the North America (<http://www-air.larc.nasa.gov/missions/TOLNet/>). The
96 primary purposes of the instruments within TOLNet are to provide regular, high-fidelity profile
97 measurements of ozone within the troposphere for satellite and model evaluation. This lidar also
98 operates routinely for the Network for the Detection of Atmospheric Composition Change (NDACC).
99 Both lidars collect backscattered radiation with a large primary telescope and a 10cm telescope for near
00 field channels. Spectral separation is accomplished using dichroic beam-splitters and interference filters.
01 For the stratospheric system, five return wavelengths are recorded: the two transmitted wavelengths,
02 and the nitrogen Raman scattered radiation from each of the transmitted beams 332 nm and 382 nm, and
03 the 408 nm water vapor channel. In this arrangement for TROLIX-19, the tropospheric system pumped
04 the Raman cell with the fourth harmonic (266 nm), which resulted in conversion to 289 nm and 299 nm
05 using a single hydrogen/deuterium Raman cell. All of the signals are further split to improve the
06 dynamic range of the respective lidar optical detection chains and are then amplified, discriminated and
07 recorded using photon counting techniques.

08 During TROLIX-19, the STROZ-LITE was operated on cloud free nights, with measurements lasting
09 between 2-4 hours to obtain enough signal to properly retrieve the entire stratospheric ozone profile.
10 The TROPOZ was operated during daytime and night time to provide tropospheric ozone profiles. For



11 instances of TROPOMI overpasses, campaign ozonesondes, or coincident stratospheric ozone lidar
12 measurements, the TROPOZ reported data is averaged for 30 minutes, centered around the satellite
13 overpass or launch time. This temporal period of averaging has been optimized in several cases to avoid
14 cloud contamination. For all other times during the TROPOZ operation, the data has been averaged to
15 10 minutes, which is suitable under most clear sky conditions to retrieve ozone information within the
16 entire troposphere.

17 **2.2 Ground Based Passive Sensors and Ozonesondes**

18 **2.2.1 Pandora Spectrometer Instrument**

19 A Pandora spectrometer instrument (#118) has been used to measure columnar amounts of trace gases
20 in the atmosphere at 3–5-minute resolution at the Cabauw site since 2016 and previously used for the
21 second Cabauw Intercomparison of Nitrogen Dioxide (CINDI-2) campaign (Kreher et al., 2020b).
22 Using the theoretical solar spectrum as a reference, Pandora determines trace gas amounts using
23 differential optical absorption spectroscopy (DOAS). This attributes in principal these differences in
24 spectra measured by Pandora to the presence of trace gases within the atmosphere (*i.e.* the difference
25 between the theoretical solar spectrum and measured spectrum is caused by absorption of trace gas
26 species). For this study, L2 direct sun columnar values of ozone are used, although retrievals of nitrogen
27 dioxide are also operationally acquired. Data used passed the strictest QC/QA estimate (Flags = 10) and
28 was obtained from the Pandonia Global Network (<http://data.pandonia-global-network.org/>).



29 **2.2.2 Brewer MKIII Spectrophotometer**

30 A Brewer MKIII spectrometer instrument (#189) has been used to measure daily columnar amounts of
31 ozone in the atmosphere at the KNMI/De Bilt (30km NE of Cabauw) site since 2007. The Brewer is
32 specifically designed to provide high accuracy measurement of spectrally resolved UV for satellite
33 evaluation, climatology monitoring and public health to international standards. Similar to Pandora
34 spectrometers, these measurements of total column of trace gases are compared to the measured UV
35 spectrum with the known solar output, and modeling the scattering properties of the atmosphere and
36 have been historically used to evaluate columnar satellite products (McPeters *et al.*, 2007; Wenig *et al.*,
37 2008; Garane *et al.*, 2019). The Brewer is the standard instrument used in the [World Meteorological](#)
38 [Organization](#) ozone monitoring network and for NDACC. This data was obtained at the NDACC
39 website (<https://www-air.larc.nasa.gov/missions/ndacc/data.html>).

40 **2.2.3 Ozonesondes**

41 Ozonesondes have been used to measure vertical profiles of ozone in the atmosphere at the KNMI/De
42 Bilt (30km NE of Cabauw) site since November 1992, and measurements are made weekly, historically
43 at 12 UTC on Thursdays. Description of the Electro Chemical Cell (ECC) details and metadata are
44 summarized in Malderen *et al.*, 2016, which also describes the importance of understanding and
45 reporting changes in ozonesonde operation procedures. During the campaign, in situ measurements of
46 ozone were made using a balloon-borne payload consisting of an ECC ozonesonde (Science Pump
47 Corporation) coupled with a radiosonde and have been used to evaluate TROPOMI tropospheric ozone
48 products in the tropics (Hubert *et al.*, 2021). The ECC technique is widely used for the high vertical



49 resolution measurements of O₃. The ECC consists of two chambers with platinum electrodes immersed
50 in potassium iodide (KI) solutions at different concentrations. The accuracy in the O₃ concentration
51 measured by an ECC ozonesonde is ± 5%–10% up to an altitude of 30 km (Smit et al., 2007). This data
52 was obtained at the NDACC website (<https://www-air.larc.nasa.gov/missions/ndacc/data.html>).

53 **2.3 Satellite Observations and Products**

54 Satellite data used in this work was selected based on the closest retrieval (*i.e.* column, profile) to the
55 CESAR station within +/-2.5 degrees latitude and +/-10 degrees in longitude.

56 **2.3.1 Ozone Mapping and Profiling Suite (OMPS) and MERRA-2 products**

57 Daily total column ozone overpasses over Cabauw station from the Ozone Mapping and Profiling Suite
58 (OMPS) Nadir-Mapper (NM) instrument on the Suomi National Polar-orbiting Partnership (S-NPP)
59 platform are used in this study. The vertical distribution of ozone in the stratosphere and lower
60 mesosphere is obtained from the OMPS Limb-Profiler (LP) sensor on the Suomi-NPP satellite merging
61 the UV (29.5–52.5 km) and VIS (12.5–35.5 km) bands to provide a full profile from 12.5 km to 52.5 km
62 (Kramarova *et al.*, 2018). Variations of this merged OMPS-LP retrieval were considered, however the
63 work shown in Arosio *et al.*, 2018, indicates the same overall conclusions would be reached. Further
64 work beyond this manuscript may involve comparing this TROLIX-19 measurement data set to specific
65 experimentally performed satellite retrievals.

66 The Modern-Era Retrospective analysis for Research and Applications, Version 2 (MERRA-2) provides
67 data beginning in 1980 and since August 2004 assimilates NASA's satellite ozone profile observations



68 from Aura Microwave Limb Sounder (MLS) (Livesey et al, 2008) to more comprehensively
69 characterize stratospheric ozone abundance. A residual tropospheric ozone product (Ziemke *et al.*,
70 2019) is derived using the OMPS NM total column ozone minus the co-located MERRA-2 stratospheric
71 column ozone. Tropopause pressure is derived from MERRA-2 potential vorticity (2.5 PVU) and
72 potential temperature (380 K).

73 **2.3.3 MLS**

74 NASA's Aura Microwave Limb Sounder (MLS) uses microwave emission to measure stratospheric
75 and upper tropospheric constituents, such as ozone. Ozone data (v5) used in this study is binned on
76 various vertical grids and are converted from volume mixing ratio to number density using the
77 coincident MERRA-2 atmosphere state parameters. Both daytime and nighttime data are used in this
78 study and the corresponding closest profile is utilized for comparison.

79 **2.3.4 TROPOMI**

80 In October 2017, the Sentinel-5 Precursor (S5P) mission was launched, carrying the TROPOspheric
81 Monitoring Instrument (TROPOMI), which is a nadir-viewing 108° Field-of-View push-broom grating
82 hyperspectral spectrometer. Starting in August 2019, Sentinel-5P TROPOMI along-track high spatial
83 resolution (approximately 5.5 km at nadir) has been implemented and total ozone columns values used
84 in this work are subsetted from the NASA GES DISC
85 (https://tropomi.gesdisc.eosdis.nasa.gov/data/S5P_TROPOMI_Level2/S5P_L2__O3_TOT_HiR.1/) to
86 provide the Offline 1-Orbit L2 (S5P_L2__O3_TOT_HiR), which is based on the Direct-fitting



87 algorithm (S5P_TO3_GODFIT), comprising a non-linear least squares inversion by comparing the
88 simulated and measured backscattered radiances.

89 Tropospheric Ozone vertical profiles were retrieved using the TOPAS (Tikhonov regularized Ozone
90 Profile retrieval with SCIATRAN) algorithm and were applied to the TROPOMI L1B spectral data
91 version 2, using spectral data between 270 and 329 nm for the retrieval (Mettig *et al.*, 2021). This data
92 set will cover the TROLIX-19 period from 09 September until 28 September; however, it is available
93 outside of this work for specific weeks between June 2018 and October 2019. Since the ozone profiles
94 are very sensitive to absolute calibration at short wavelengths, a re-calibration of the measured
95 radiances is required using comparisons with simulated radiances with ozone limb profiles from
96 collocated satellites used as input. The a priori profiles for ozone are taken from the ozone climatology
97 of Lamsal *et al.* (2004) and the calibration correction spectrum is determined using the radiances
98 modelled with ozone information from collocated MLS/Aura measurements as described in depth
99 throughout Mettig *et al.*, 2021.

00

01 **2.4 Coupled Chemistry and Meteorology Model**

02 The GEOS Composition Forecasting (GEOS-CF,
03 https://gmao.gsfc.nasa.gov/weather_prediction/GEOS-CF/, Keller *et al.*, 2021, Knowland *et al.*, 2021)
04 system was chosen to serve as a comparison simulation for this effort, based on its altitude coverage (up
05 to 80 km) and implications for future geostationary satellite use. The system produces global, three-
06 dimensional distributions of atmospheric composition with a spatial resolution of 25km. Using
07 meteorological analyses from other GEOS systems, the GEOS-CF products include a running



08 atmospheric replay to provide near-time estimates of surface pollutant distributions and the composition
09 of the troposphere and stratosphere. Individual case study evaluations using ozone lidar of the GEOS-
10 CF meteorological replay have recently been performed in Dacic et al. (2020), Gronoff et al. (2021) and
11 Johnson et al. (2021). These results will also be used to better evaluate the GEOS-CF as the source of a
12 priori ozone profiles for use in the TEMPO tropospheric ozone retrievals. Model output for this work is
13 used from the closest GEOS-CF model grid cell to the CESAR observatory.

14 **3 Tropospheric Ozone Comparisons**

15 **3.1 Vertical Profiles**

16 Example tropospheric ozone profile observations are presented in **Figure 2** for 7 individual observation
17 periods during the TROLIX-19 campaign. Each of the panels show the cloud screened TROPOZ lidar
18 retrievals (top panels) and the corresponding GEOS-CF model output (bottom panels). Pink dots are
19 overlaid to indicate the simulated tropopause altitude based on a blended estimate (TROPPB) which
20 meets criteria of the lowest altitude bin corresponding with either a pressure level above the thermal
21 tropopause (380K) or dynamical (3 PVU) tropopause.

22 In general, the observations and simulations agree quite well in characterizing the broad features that
23 impacted the CESAR site during the TROLIX-19 campaign. However, in each panel there are ozone
24 laminae within the lower troposphere that are not replicated in the model simulation, most notably
25 during the September 20-21 period (Figure 2d-e). The observations indicate increased ozone levels as
26 compared to the model during this period, centered around the 3-5km and 8-10km region of the



27 atmosphere (this is explored in more detail below). However, the model does simulate well the lowered
28 tropopause height and abundance of lower stratospheric ozone observed in the 2 October observations
29 (see Fig. 2g), which is an indication of the model well representing the dynamical variability that affects
30 the lowering of the tropopause height.

31 To bring in additional platforms and to better understand these differences throughout the campaign at
32 discrete altitudes, **Figure 3** shows the ozone number density values for the TROPOZ lidar, GEOS-CF
33 model, TROPOMI and ECC ozonesondes at the 4 km vertical level for the entire TROLIX-19 campaign
34 period. Within the 4km layer, the platforms are all characterizing the general ozone features throughout
35 the campaign at an altitude that frequently is associated with aged transported layering. There is a
36 noticeable difference between the observations and model during the previously described 20-21
37 September period. On 21 September at 12 UT, the lidar and ECC sonde quantify an elevated layer (1.2-
38 1.3×10^{21} molecules m^{-3}) into the region that is not simulated by model ($0.75-0.9 \times 10^{21}$ molecules m^{-3}),
39 resulting in an approximately 30% difference in ozone abundance within layer. Since the model
40 correctly simulated many other ozone features during this time period within the upper tropospheric
41 region, this is likely aged transport into the domain that was not available during model initialization.
42 Back-trajectories were performed to better identify the source of this air mass, however nothing
43 conclusive can be reported. The layer is not associated with any increase in lidar attenuated backscatter
44 within the associated altitude, suggesting it was not urban in origin and therefore more likely aged
45 stratospheric air mixing down to the lower free troposphere. Outside of this Sep 21 period, there is
46 generally good agreement between the observations and model, indicating the combination of



47 observations and modeling are able to represent the rural conditions and ozone perturbations at the
48 CESAR site.

49 **3.2 Columnar Data Reduction**

50 There continues to be a need within the atmospheric and satellite community to understand the
51 variability of ozone as it pertains to both the tropospheric column (*i.e.* the Earth's surface to the
52 tropopause height) and the 0-2km tropospheric column (*i.e.* the Earth's surface to the 2 km height). The
53 0-2 km region is of particular interest as it is projected to be delivered hourly from the North American
54 geo-stationary satellite: Tropospheric Emissions: Monitoring of Pollution (TEMPO). Due to the
55 increased temporal frequency and vertical extent of TEMPO's tropospheric ozone retrievals, ozone
56 lidars, such as those from TOLNet (<https://www-air.larc.nasa.gov/missions/TOLNet/>) used in this work,
57 are an ideal platform to perform future evaluations of the products, which build from Johnson *et al.*,
58 2018.

59 Full tropospheric columns (**Figure 4, top panel**) are consistently calculated from each platform using
60 the blended tropopause height (TROPPB) produced by the GEOS-CF and described above (*c.f.* pink
61 dots in **Figure 2**) and are then converted to Dobson Units (DU). The tropospheric columns are
62 calculated explicitly by integrating the ozone number density from the lowest data bin of usable data to
63 the TROPPB produced in the nearest model temporal output. The exception to this is the
64 OMPS/MERRA-2 tropospheric column using the residual method described above (subtracting the
65 MERRA-2 stratospheric column from the OMPS-NM total ozone column). For the 0-2km tropospheric



66 column (**Figure 4, bottom panel**), there were no major surface layer pollution events at the CESAR
67 observatory during TROLIX-19.

68 For the full tropospheric column (Figure 4, top panel), the campaign variability ranges from
69 approximately 20-55 DU. The model, lidar, and ECC sonde observations agree quite well throughout
70 the 12 Sep to 23 Sep time frame when looking at day-to-day variability. However, when assessing the
71 variability on a single day for 21 Sep, full tropospheric columns reduced from the lidar observations are
72 some of the largest observed during this TROLIX-19 period (reaching nearly 50 DU), while the model
73 mainly ranges between 35-37 DU or a difference of upwards of 40%. Therefore, this increase identified
74 and discussed in Fig 3, not only results an altitude specific difference, but ultimately results in a large
75 overall impact to the full tropospheric column content. This suggests ground-based profiling
76 observations are still critically needed to confirm large deviations from a priori and climatology in order
77 to evaluate the atmospheric chemistry models.

78 There exists both diurnal and day-to-day variability of the 0-2 km ozone, ranging from 4-10 DU
79 (Figure 4, top panel). In the 0-2 km ozone reduction, the lidar and model are critically needed to
80 understand ozone variability on a continuous scale. For instance, on 15 Sep the 0-2 km ozone column
81 was near 9 DU at 03 UT and finished near 5.5 DU at 16 UT, resulting in a -60% change in DU within a
82 single day. Furthermore, the gradient of the 21 Sep ozone column change was similar in scale to the
83 entire campaign variability, indicating that there is a significant amount of information gained in the
84 understanding of the variability in ozone from continuous measurements. Although a daily snapshot of
85 OMPS-MERRA-2 residuals and TROPOMI ozone profile observations are critical for their vast spatial



86 coverage, ground-based observations such as ozone lidar and ECC sondes are critically needed to
87 quantify measurement gaps.

88 In summary, we find that the ozone columns evaluated in this study generally reproduced the structure
89 of the TROLIX-19 ozone lidar observations for N=835 coincidences. For the full tropospheric column,
90 the lidar calculated median was 30.9 ± 4.7 DU, compared to 33.4 ± 3.9 DU for the GEOS-CF. This
91 indicates a difference of 2.5 DU or 7.9 %, which is well within the lidar uncertainty of around 10 %
92 throughout the tropospheric column, and as we described above is likely driven by select days rather
93 than an overall bias between the measurements.. For the 0-2 km tropospheric column, the lidar
94 calculated median was $5.8 \text{ DU} \pm 0.9 \text{ DU}$, compared to $6.9 \text{ DU} \pm 0.7 \text{ DU}$ for the corresponding GEOS-
95 CF measurements. This indicates a difference between observations and model of 1.1 DU or 18.9 %,
96 which is higher than the lidar uncertainty of around 5-10 % throughout the column. For the TROLIX-19
97 campaign, a 0-2 km tropospheric column accounts for approximately 20% of the tropospheric column
98 as detailed in Figure 4 (top panel), indicating measurements above the surface are critically needed at
99 understanding ozone variability at rural sites such as Cabauw, NL, where free tropospheric ozone
00 features dominate the column.

01 **4 Full Profile Ozone Comparisons**

02 **4.1 Hybrid Tropospheric/Stratospheric Ozone Comparisons**

03 To better understand differences in ozone retrievals from multiple platforms, it is important to assess the
04 entire vertical distribution of ozone. To characterize the vertical distribution throughout the entire



05 troposphere and stratosphere, hybrid ozone profiles were created from longer (integrations of 60-120
06 minute vs 10 minutes in Sec 3) temporal retrievals from the co-located TROPOZ and STROZ lidars,
07 which were then interpolated to the GEOS-CF model vertical grid levels. **Figure 5** compares these
08 results to the GEOS-CF, OMPS-LP, TROPOMI, MLS and the ECC ozonesonde profiles for 12 Sep, 17
09 Sep, 19 Sep, and 21 Sep 2019. These days were selected as days within the campaign that had an ECC
10 launch from De Bilt, NL (30 km from Cabauw).

11 For each observation period in **Figure 5**, all platforms manage to characterize a similar shape and extent
12 of the ozone maxima between 2.5-4.5 molecules m⁻³ throughout the vertical layer between 20-25 km. In
13 each case, there are differences between the platforms in characterizing the vertical variability and
14 extent of the ozone maxima, which will be quantified in the following section. One notable feature that
15 emphasizes the cross-platform ability to illustrate ozone variability in the stratosphere is from the 19
16 and 21 Sep profiles. A dual ozone maximum is observed quite remarkably by the merged lidar, ECC,
17 MLS, OMPS-LP and simulated by the GEOS-CF centered around 20 km and then again at 25km. The
18 wind observations from the ozonesonde payload (not shown) indicate a wind shear within the two ozone
19 layers, suggesting this feature was dynamically driven. The TROPOMI retrieval is not able to retrieve
20 this vertical features due to its coarser vertical resolution and appears to average through the layers.

21 **4.2 Difference Profiles**

22 To quantitatively compare the ozone retrievals and simulations, **Figure 6** displays the ozone
23 values for the TROLIX-19 time period from the hybrid lidar dataset (**Figure 6a**), GEOS-CF (**Figure**
24 **6b**), OMPS-LP (**Figure 6c**), MLS (**Figure 6d**) and TROPOMI (**Figure 6e**). This double ozone maxima,



25 starting after 20 September serves as a geophysical marker to visually compare the ozone products. The
26 lidar, model, and OMPS-LP all capture this feature, but with varying ozone abundances and altitudes.
27 From **Figure 6d**, it appears as if TROPOMI retrievals are not able to resolve this feature. The percent
28 differences, as compared to the lidar observations, are displayed in **Figure 7a-d**. These percent
29 differences are calculated using (1)

30

$$31 \quad (1) \text{ Percent Difference} = \frac{(E_1 - E_2)}{\frac{1}{2}(E_1 + E_2)} \times 100$$

32

33

34 where E_2 are the lidar observations and E_1 are the respective ozone values from the various platforms in
35 **Figure 6**.

36 The percent differences in **Figure 7a** indicate the GEOS-CF model from 20-45 km generally represents
37 the lidar observations, but are generally 0-10 % lower in abundance. The percent differences in **Figure**
38 **7b** indicate OMPS-LP is also representing the ozone maxima and altitude above 25 km. There are larger
39 differences below 20 km, which indicates the OMPS-LP retrieval is generally underestimating the ozone
40 abundance below 20 km as shown in the profiles in **Figure 5**. The percent differences in **Figure 7c**
41 indicate the MLS data, especially that within the 20-40km region, perform quite well as compared to the
42 lidar observations. The percent differences in **Figure 7d** indicate the TROPOMI retrieval is generally
43 over representing the ozone concentrations throughout the atmosphere, which worsens within the
44 troposphere. In all cases, the most variability in the differences occur within the active region from 10-
45 20 km that is driven by the dynamical tropopause height and lower stratospheric ozone abundance.



46 **5 Total Column Ozone**

47 Similar to the troposphere, to better understand to what extent the vertical distribution of ozone impacts
48 the atmospheric column, **Figure 8 (top panel)** shows the various platforms and their retrieved total
49 column ozone. For this analysis, the GEOS-CF, lidar, OMPS-NM, TROPOMI (GODFIT) are shown, in
50 addition to local ground-based measurements from a Pandora instrument and Brewer. The total column
51 values range from 230-300 DU throughout the campaign period, with the median total column ozone of
52 271 DU. With the previous analyses from Sec 3.2, this indicates the median total tropospheric column
53 of 33 DU and 0-2km boundary layer column of 6 DU result in percentages of the entire ozone column
54 of 12% and 2.3%, respectively. Similar to the full tropospheric ozone columns, larger total ozone
55 columns were observed towards the end of the TROLIX-19 period, suggesting this variability was
56 partly due to a larger abundance of ozone in the lower stratosphere.

57 **Figure 8 (bottom panel)** shows the various platforms as a percent differences from the model. In
58 general, the various platforms are all within 10 % of each other, with most differences being within
59 $\pm 5\%$. This analysis emphasizes the stability and maturity of the Pandora and Brewer systems for
60 monitoring the total column ozone amounts. Interestingly, the double maxima feature in vertical ozone
61 distribution in the stratosphere (with local minima between) described in Sec 4.1 on 21 Sep does not
62 severely impact the total column ozone.

63 **6 Conclusions**

64 This work has highlighted the various differences in retrieved ozone quantities during the TROLIX-19
65 campaign. This has emphasized the importance of ground-based ozone lidars and other measurements



66 in understanding the vertical variability of ozone and how it relates to the column reduction. This work
67 also shows the first effort to directly resolve both tropospheric columns and 0-2km ozone columns from
68 the NASA TROPOZ lidar. Other TOLNet lidars are able to perform this data reduction and future work
69 will be to expand this effort to the other TOLNet locations. This work indicates the level of
70 performance of the GEOS-CF modeling system as compared to the other platforms, which ultimately
71 performs extremely well both in the stratosphere and within the troposphere, as emphasized in **Figure 6**
72 and **Figure 7**. In looking towards the NASA TEMPO mission, this work indicates that the GEOS-CF is
73 an appropriate choice for the a priori profiles for the TEMPO ozone retrievals. This work shows the
74 TROPOMI ozone profile products are able to accurately reproduce ozone quantities in the lower
75 troposphere at various atmospheric levels. In particular, **Figure 3** shows promising results that indicate
76 the TROPOMI satellite observations compare well with the observations from ground-based
77 measurements (lidar, sonde) of specific elevated ozone features.

78 The CESAR Observatory continues to be a critical landmark for campaigns that revolve around
79 atmospheric composition measurements for satellite validation and evaluation beyond this effort, such
80 as CINDI and CINDI-2 (Kreher *et al.*, 2020; Tirpitz *et al.*, 2021). As the European Commission (EC) in
81 partnership with the European Space Agency (ESA) continues to launch tropospheric composition
82 satellites, including the upcoming geo-stationary Sentinel-4 satellite, we expect this observatory will
83 continue to host and maintain critical atmospheric sampling for future validation efforts.

84

85

86



87 Data Availability.

88

89 1. MLS ozone profiles can be downloaded from the NASA Goddard Space Flight Center Earth
90 Sciences Data and Information Services Center (GES DISC; Schwartz et al., 2020,
91 <https://doi.org/10.5067/Aura/MLS/DATA2516>, last access: 29 March 2022).

92 2. The Pandora data is available at the Pandonia Global Network Archive ([http://data.pandonia-
93 global-network.org/Cabauw/](http://data.pandonia-global-network.org/Cabauw/), last access 29 March 29, 2022).

94 3. The OMPS LP version 2.5 ozone profiles can be downloaded from the NASA Goddard Space
95 Flight Center Earth Sciences Data and Information Services Center (GES DISC;
96 at <https://doi.org/10.5067/X1Q9VA07QDS7> (Deland, 2017, last access: 29 March 2022).

97 4. The tropospheric ozone lidar data used in this publication were obtained from the Cabauw
98 Experimental Site for Atmospheric Research (CESAR) as part of a campaign involving the
99 Network for the Detection of Atmospheric Composition Change (NDACC) and NASA's
00 Tropospheric Ozone Lidar Network (TOLNet) and are publicly available ([https://www-
01 air.larc.nasa.gov/cgi-bin/ArcView.1/TOLNet?NASA-GSFC=1](https://www-air.larc.nasa.gov/cgi-bin/ArcView.1/TOLNet?NASA-GSFC=1), last access: 29 March 2022).

02 5. The ozonesonde and Brewer data used in this publication were obtained from the De Bilt, NL
03 site as part of a campaign involving the Network for the Detection of Atmospheric Composition
04 Change (NDACC) and are publicly available (<ftp://ftp.cpc.ncep.noaa.gov/ndacc/station/debilt/>,
05 last access: 29 March 2022).

06 6. The stratospheric ozone lidar data used in this publication were obtained from the Cabauw
07 Experimental Site for Atmospheric Research (CESAR) as part of a campaign involving the



- 08 Network for the Detection of Atmospheric Composition Change (NDACC) and are publicly
09 available (<ftp://ftp.cpc.ncep.noaa.gov/ndacc/station/cabauw/>, last access: 29 March 2022).
- 10 7. The TROPOMI TOPAS Ozone Profile data and source codes are available upon request from
11 Nora Mettig (mettig@iup.physik.uni-bremen.de) or Mark Weber (weber@uni-bremen.de). The
12 L1B version of the S5P data is available upon request to the S5P Validation Team.
- 13 8. The Tropospheric Ozone Column from OMPS-NM/MERRA-2 Daily measurements data are
14 available upon request from Jerry Ziemke (Jerald.r.ziemke@nasa.gov).
- 15 9. The NASA GEOS-CF simulations are available at the data sharing portal
16 (<https://portal.nccs.nasa.gov/datashare/gmao/geos-cf/v1/forecast/>, last access 29 March 2022).
- 17
- 18 Author contributions. JS drafted the original manuscript. JS, LT, GS, and TM deployed and operated
19 the NASA ozone lidars and provided expertise on use of measurements. NM, AR, and MW provided
20 TOPAS ozone profile data and guidance on how best to use the measurements. AA and KK provided
21 overall context as principal investigators of the TROLIX-19 campaign and coordinated science team
22 meetings to foster this collaboration. KEK provided GEOS-CF data and insight on its use in this work.
23 MA, AP, MvR, and PV provided expertise and data for the ground-observations for ozonesondes,
24 Brewer, and historical data for the Cabauw site. JZ provided data for the OMPS-MERRA-2
25 tropospheric column data. NK provided Aura MLS, OMPS-LP merged data and further insight into the
26 use of the data.
- 27
- 28 Competing interests. The authors declare that they have no conflict of interest.



29

30 Disclaimer. Publisher's note: Copernicus Publications remains neutral with regard to jurisdictional
31 claims in published maps and institutional affiliations.

32

33 Acknowledgements. NASA data has been provided through the Tropospheric Composition and Upper
34 Atmosphere Research Programs. We acknowledge all additional data providers and their funding
35 agencies for performing regular measurements and retrievals.

36

37

38

39 References

40

41 Apituley, Arnoud, Karin Kreher, Michael Van Roozendael, John Sullivan, Thomas J. McGee, Marc
42 Allaart, Ankie Piters et al. "Overview of activities during the 2019 TROPomi vaLIdation eXperiment
43 (TROLIX'19)." In *AGU Fall Meeting Abstracts*, vol. 2019, pp. A43J-2958. 2019

44

45 Apituley, Arnoud, Karin Kreher, Ankie Piters, John Sullivan, Michel vanRoozendael, Tim Vlemmix,
46 Mirjam den Hoed et al. "Overview of the 2019 Sentinel-5p TROPomi vaLIdation eXperiment
47 (TROLIX)." In *EGU General Assembly Conference Abstracts*, p. 10539. 2020.

48

49 Arosio, Carlo, Alexei Rozanov, Elizaveta Malinina, Kai-Uwe Eichmann, Thomas von Clarmann, and
50 John P. Burrows. "Retrieval of ozone profiles from OMPS limb scattering observations." *Atmospheric
51 Measurement Techniques* 11, no. 4 (2018): 2135-2149.

52

53 Copernicus Sentinel data processed by ESA, German Aerospace Center (DLR) (2019), Sentinel-5P
54 TROPOMI Total Ozone Column 1-Orbit L2 5.5km x 3.5km, Greenbelt, MD, USA, Goddard Earth
55 Sciences Data and Information Services Center (GES DISC), Accessed: [10 December 2021],

56

[10.5270/S5P-fqouvyz](https://doi.org/10.5270/S5P-fqouvyz)

57



- 58 Dacic, Natasha, John T. Sullivan, K. Emma Knowland, Glenn M. Wolfe, Luke D. Oman, Timothy A.
59 Berkoff, and Guillaume P. Gronoff. "Evaluation of NASA's high-resolution global composition
60 simulations: Understanding a pollution event in the Chesapeake Bay during the summer 2017 OWLETS
61 campaign." *Atmospheric Environment* 222 (2020): 117133.
62
- 63 Garane, Katerina, Maria-Elissavet Koukouli, Tijn Verhoelst, Christophe Lerot, Klaus-Peter Heue, Vitali
64 Fioletov, Dimitrios Balis et al. "TROPOMI/S5P total ozone column data: global ground-based
65 validation and consistency with other satellite missions." *Atmospheric Measurement Techniques* 12, no.
66 10 (2019): 5263-5287.
67
- 68 Gronoff, G., T. Berkoff, K. E. Knowland, L. Lei, M. Shook, B. Fabbri, W. Carrion, and A. O. Langford.
69 "Case study of stratospheric Intrusion above Hampton, Virginia: lidar-observation and modeling
70 analysis." *Atmospheric Environment* (2021): 118498.
71
- 72 Hubert, Daan, Klaus-Peter Heue, Jean-Christopher Lambert, Tijn Verhoelst, Marc Allaart, Steven
73 Compernelle, Patrick D. Cullis et al. "TROPOMI tropospheric ozone column data: geophysical
74 assessment and comparison to ozonesondes, GOME-2B and OMI." *Atmospheric Measurement
75 Techniques* 14, no. 12 (2021): 7405-7433.
76
- 77 Johnson, M. S., Liu, X., Zoogman, P., Sullivan, J., Newchurch, M. J., Kuang, S., Leblanc, T., and
78 McGee, T.: Evaluation of potential sources of a priori ozone profiles for TEMPO tropospheric ozone
79 retrievals, *Atmos. Meas. Tech.*, 11, 3457–3477, <https://doi.org/10.5194/amt-11-3457-2018>, 2018.
80
- 81 Keller, Christoph A., K. Emma Knowland, Bryan N. Duncan, Junhua Liu, Daniel C. Anderson, Sampa
82 Das, Robert A. Lucchesi et al. "Description of the NASA GEOS Composition Forecast Modeling
83 System GEOS-CF v1. 0." *Journal of Advances in Modeling Earth Systems* 13, no. 4 (2021):
84 e2020MS002413.
85
- 86 Kramarova, Natalya A., Pawan K. Bhartia, Glen Jaross, Leslie Moy, Philippe Xu, Zhong Chen,
87 Matthew DeLand et al. "Validation of ozone profile retrievals derived from the OMPS LP version 2.5
88 algorithm against correlative satellite measurements." *Atmospheric Measurement Techniques* 11, no. 5
89 (2018): 2837-2861.
90
- 91 Kreher, Karin, Michel Van Roozendael, Francois Hendrick, Arnoud Apituley, Ermioni Dimitropoulou,
92 Udo Frieß, Andreas Richter et al. "Intercomparison of NO₂, O₄, O₃ and HCHO slant column
93 measurements by MAX-DOAS and zenith-sky UV–visible spectrometers during CINDI-2."
94 *Atmospheric Measurement Techniques* 13, no. 5 (2020): 2169-2208.
95
- 96 Lamsal, L. N., M. Weber, S. Tellmann, and J. P. Burrows. "Ozone column classified climatology of
97 ozone and temperature profiles based on ozonesonde and satellite data." *Journal of Geophysical
98 Research: Atmospheres* 109, no. D20 (2004).
99



- 00 Leblanc, Thierry, Mark A. Brewer, Patrick S. Wang, Maria Jose Granados-Muñoz, Kevin B.
01 Strawbridge, Michael Travis, Bernard Firanski et al. "Validation of the TOLNet lidars: the Southern
02 California Ozone Observation Project (SCOOP)." *Atmospheric measurement techniques* 11, no. 11
03 (2018): 6137-6162.
04
- 05 Livesey, N. J., M. J. Filipiak, L. Froidevaux, W. G. Read, A. Lambert, M. L. Santee, J. H. Jiang et al.
06 "Validation of Aura Microwave Limb Sounder O₃ and CO observations in the upper troposphere and
07 lower stratosphere." *Journal of Geophysical Research: Atmospheres* 113, no. D15 (2008).
08
- 09 Malderen, Roeland Van, Marc AF Allaart, Hugo De Backer, Herman GJ Smit, and Dirk De Muer. "On
10 instrumental errors and related correction strategies of ozonesondes: possible effect on calculated ozone
11 trends for the nearby sites Uccle and De Bilt." *Atmospheric Measurement Techniques* 9, no. 8 (2016):
12 3793-3816.
13
- 14 McGee, Thomas J., David N. Whiteman, Richard A. Ferrare, James J. Butler, and John F. Burris.
15 "STROZ LITE: stratospheric ozone lidar trailer experiment." *Optical Engineering* 30, no. 1 (1991): 31-
16 39.
17
- 18 McPeters, Richard D., Gordon J. Labow, and Jennifer A. Logan. "Ozone climatological profiles for
19 satellite retrieval algorithms." *Journal of Geophysical Research: Atmospheres* 112, no. D5 (2007).
20
- 21 Mettig, N., Weber, M., Rozanov, A., Arosio, C., Burrows, J. P., Veefkind, P., Thompson, A. M.,
22 Querel, R., Leblanc, T., Godin-Beekmann, S., Kivi, R., and Tully, M. B.: Ozone profile retrieval from
23 nadir TROPOMI measurements in the UV range, *Atmos. Meas. Tech.*, 14, 6057–6082,
24 <https://doi.org/10.5194/amt-14-6057-2021>, 2021.
25
- 26 Mettig, Nora, Mark Weber, Alexei Rozanov, John P. Burrows, Pepijn Veefkind, Nadia Smith, Anne M.
27 Thompson et al. "Combined UV and IR ozone profile retrieval from TROPOMI and CrIS
28 measurements." *Atmospheric Measurement Techniques Discussions* (2021): 1-33.
29
- 30 Piters, A. J. M., Boersma, K. F., Kroon, M., Hains, J. C., Van Roozendaal, M., Wittrock, F., Abuhassan,
31 N., Adams, C., Akrami, M., Allaart, M. A. F., Apituley, A., Beirle, S., Bergwerff, J. B., Berkhout, A. J.
32 C., Brunner, D., Cede, A., Chong, J., Clémer, K., Fayt, C., Frieß, U., Gast, L. F. L., Gil-Ojeda, M.,
33 Goutail, F., Graves, R., Griesfeller, A., Großmann, K., Hemerijckx, G., Hendrick, F., Henzing, B.,
34 Herman, J., Hermans, C., Hoexum, M., van der Hoff, G. R., Irie, H., Johnston, P. V., Kanaya, Y., Kim,
35 Y. J., Klein Baltink, H., Kreher, K., de Leeuw, G., Leigh, R., Merlaud, A., Moerman, M. M., Monks, P.
36 S., Mount, G. H., Navarro-Comas, M., Oetjen, H., Pazmino, A., Perez-Camacho, M., Peters, E., du
37 Piesanie, A., Pinardi, G., Puentedura, O., Richter, A., Roscoe, H. K., Schönhardt, A., Schwarzenbach,
38 B., Shaiganfar, R., Sluis, W., Spinei, E., Stolk, A. P., Strong, K., Swart, D. P. J., Takashima, H.,
39 Vlemmix, T., Vrekoussis, M., Wagner, T., Whyte, C., Wilson, K. M., Yela, M., Yilmaz, S., Zieger, P.,
40 and Zhou, Y.: The Cabauw Intercomparison campaign for Nitrogen Dioxide measuring Instruments



- 41 (CINDI): design, execution, and early results, *Atmos. Meas. Tech.*, 5, 457–485, doi:10.5194/amt-5-457-
42 2012, 2012.
- 43
- 44 Sullivan, J. T., T. J. McGee, G. K. Sumnicht, L. W. Twigg, and R. M. Hoff. "A mobile differential
45 absorption lidar to measure sub-hourly fluctuation of tropospheric ozone profiles in the Baltimore–
46 Washington, DC region." *Atmospheric Measurement Techniques* 7, no. 10 (2014): 3529-3548.
- 47
- 48 Sullivan, John T., Thomas J. McGee, Anne M. Thompson, R. Bradley Pierce, Grant K. Sumnicht,
49 Laurence W. Twigg, Edwin Eloranta, and Raymond M. Hoff. "Characterizing the lifetime and
50 occurrence of stratospheric-tropospheric exchange events in the rocky mountain region using high-
51 resolution ozone measurements." *Journal of Geophysical Research: Atmospheres* 120, no. 24 (2015):
52 12410-12424.
- 53
- 54 Sullivan, John T., Timothy Berkoff, Guillaume Gronoff, Travis Knepp, Margaret Pippin, Danette Allen,
55 Laurence Twigg et al. "The ozone water–land environmental transition study: An innovative strategy
56 for understanding Chesapeake Bay pollution events." *Bulletin of the American Meteorological Society*
57 100, no. 2 (2019): 291-306.
- 58
- 59 Tirpitz, Jan-Lukas, Udo Frieß, François Hendrick, Carlos Alberti, Marc Allaart, Arnoud Apituley, Alkis
60 Bais et al. "Intercomparison of MAX-DOAS vertical profile retrieval algorithms: studies on field data
61 from the CINDI-2 campaign." *Atmospheric Measurement Techniques* 14, no. 1 (2021): 1-35.
- 62
- 63 Wenig, Mark O., A. M. Cede, E. J. Bucsela, E. A. Celarier, K. F. Boersma, J. P. Veefkind, E. J.
64 Brinkma, J. F. Gleason, and J. R. Herman. "Validation of OMI tropospheric NO₂ column densities
65 using direct-Sun mode Brewer measurements at NASA Goddard Space Flight Center." *Journal of*
66 *Geophysical Research: Atmospheres* 113, no. D16 (2008).
- 67
- 68 Wing, Robin, Wolfgang Steinbrecht, Sophie Godin-Beekmann, Thomas J. McGee, John T. Sullivan,
69 Grant Sumnicht, Gérard Ancellet, Alain Hauchecorne, Sergey Khaykin, and Philippe Keckhut.
70 "Intercomparison and evaluation of ground-and satellite-based stratospheric ozone and temperature
71 profiles above Observatoire de Haute-Provence during the Lidar Validation NDACC Experiment
72 (LAVANDE)." *Atmospheric Measurement Techniques* 13, no. 10 (2020): 5621-5642.
- 73
- 74 Wing, Robin, Sophie Godin-Beekmann, Wolfgang Steinbrecht, Thomas J. McGee, John T. Sullivan,
75 Sergey Khaykin, Grant Sumnicht, and Laurence Twigg. "Evaluation of the new DWD ozone and
76 temperature lidar during the Hohenpeißenberg Ozone Profiling Study (HOPS) and comparison of
77 results with previous NDACC campaigns." *Atmospheric Measurement Techniques* 14, no. 5 (2021):
78 3773-3794.
- 79
- 80 Ziemke, Jerry R., Luke D. Oman, Sarah A. Strode, Anne R. Douglass, Mark A. Olsen, Richard D.
81 McPeters, Pawan K. Bhartia et al. "Trends in global tropospheric ozone inferred from a composite



82 record of TOMS/OMI/MLS/OMPS satellite measurements and the MERRA-2 GMI simulation."
83 *Atmospheric Chemistry and Physics* 19, no. 5 (2019): 3257-3269.
84
85
86
87
88
89
90
91
92
93
94
95
96
97
98
99
00
01
02
03
04
05
06
07
08
09
10
11
12
13
14

15 **Table 1: Instrument platforms, associated products, and short description used in this work during the TROLIX-19**
16 **campaign.**

17

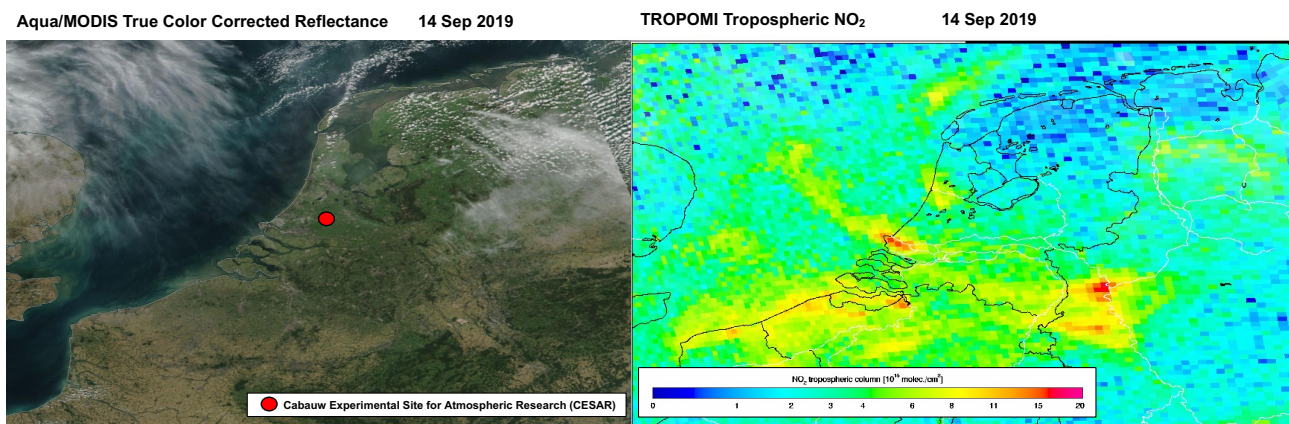
Instrument	Products	Platform	Description
GSFC TROPOZ [NASA]	Profiles [0.2 – 18 km]	Ground-based Lidar	10 min integration; 30-90-min avg around ECC or Satellite Overpass



GSFC STROZ [NASA]	Profiles [15 - 48 km]	Ground-based Lidar	~2-4-hr avg between (20-23 UT)
ECC Ozone sondes [KNMI]	Profiles [0 – 33 km]	Balloonborne	Balloonborne, Launched at 12 UT from De Bilt (~30 km from Cabauw) on 4 days
Pandora [NASA/KNMI]	Column [TCO]	Spectrometer	L2 Pandora 118s, Data Used has QC/QA Flags = 10
Brewer [KNM]	Column [TCO]	Spectrophotometer	L2 Brewer #189m, MKIII, Located in De Bilt
S5P/TropOMI [ESA]	Column [TCL]	Satellite	L2 TOPAS Product, Overpass between 12-14 UT (5.5x3.5 km, nadir)
S5P/TropOMI [KNMI]	Column [TCO]	Satellite	L2 GODFIT v4 TO3 Product, Overpass between 12-14 UT (5.5x3.5 km, nadir)
OMPS [NASA]	Column [TCO]	Satellite	L3 NM Product, Version 2, Daily Overpass between 12-14 UT (50x50 km, nadir)
OMPS-LP [NASA]	Profiles [12-60km]	Satellite	Merged L2 v2.5 Daily Merged Product, Overpass between 12-14 UT (1km vertical bins)
OMPS/MERRA-2 [NASA]	Trop. Columns	Satellite/Assimilation	L4 Derived Product, OMPS-NM daily Overpass, MERRA-2
AURA MLS [NASA]	Profiles [12-60km]	Satellite	Merged L2 v5 Daily Daytime/Nighttime Products, Overpass between 12-14 UT (1km vertical bins) and 01-03 UT.
GEOS-CF [NASA]	Profiles [0-80km]	Global 3-D CCMM	<u>1-Hr, 72 lev, Met. Replay, (25x25km)</u>



19
20
21
22
23
24
25
26
27
28
29
30
31
32
33



34
35
36
37
38
39
40

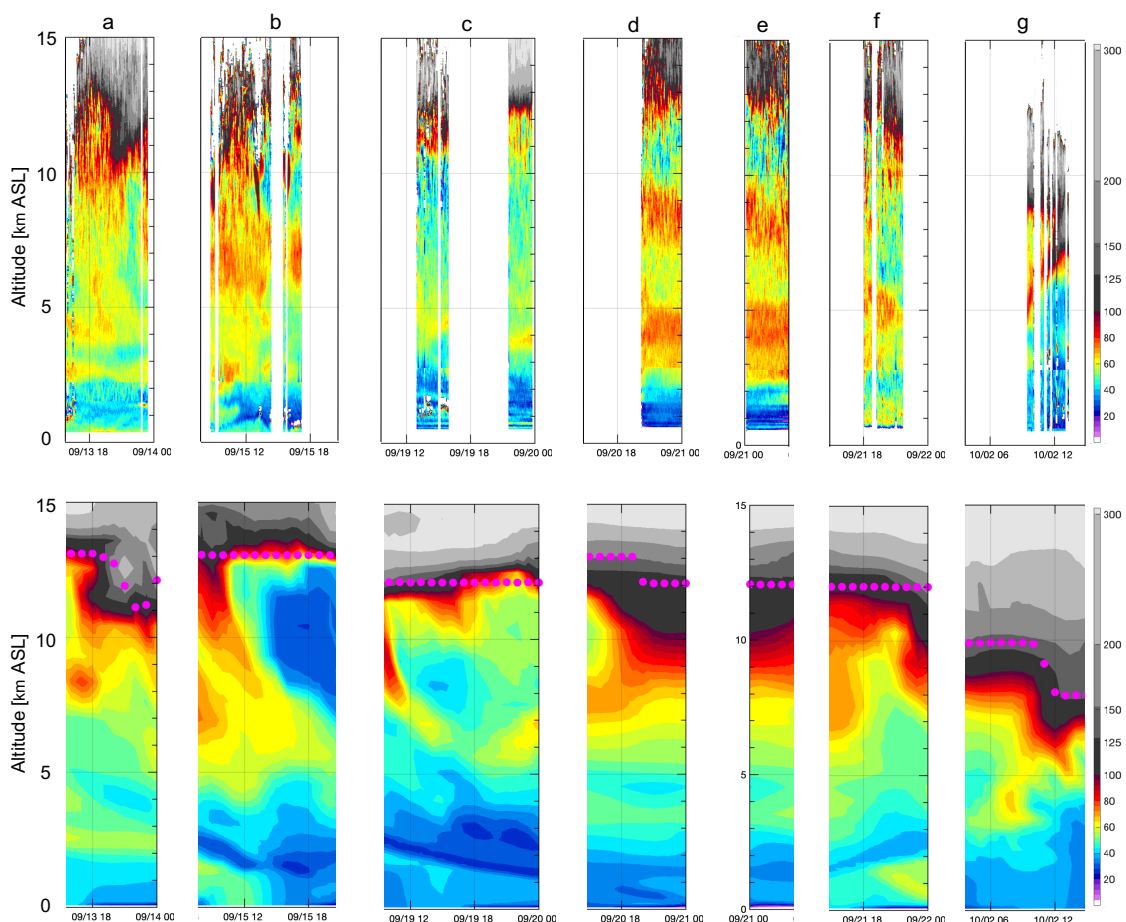
41 **Figure 1: Aqua/MODIS True Color Corrected Reflectance (left) and TROPOMI Tropospheric NO₂ (right) for 14**
42 **September 2019. The CESAR site is indicated in the image on the left.**

43
44
45
46



47
48
49

NASA GSFC Ozone Lidar and GEOS-CF Ozone at Cabauw, NL (TROLIX-19)



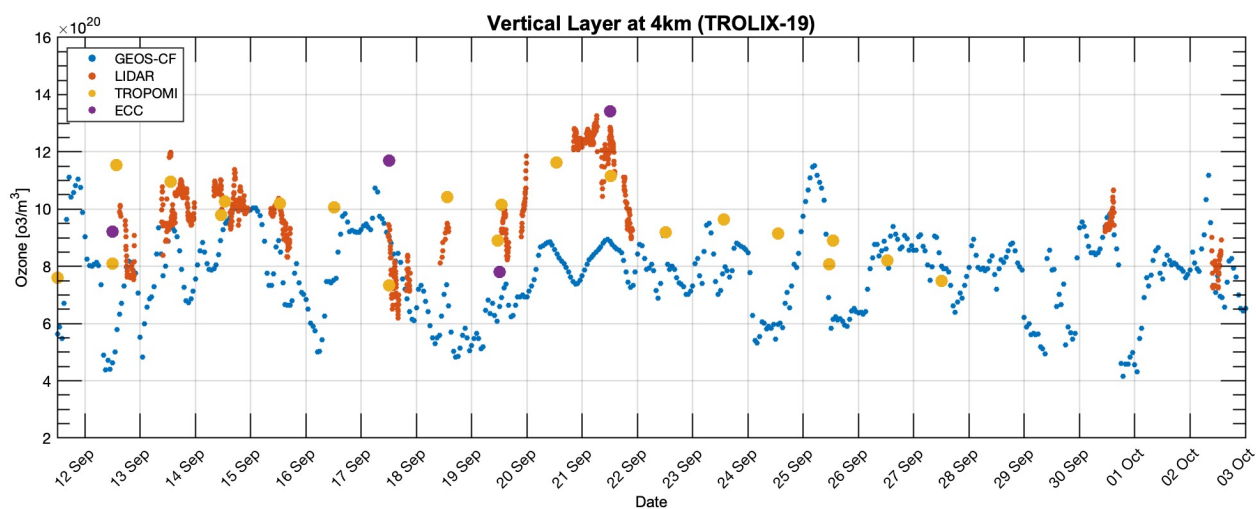
50

51 **Figure 2: Cloud screened TROPOZ lidar retrievals (top panel) and the corresponding GEOS-CF model output (bottom**
52 **panel) from the closest model grid cell to the CESAR observatory during TROLIX-19 for a) 13 Sep 14-00 UTC, b) 15**
53 **Sep 09-21 UTC, c) 19 Sep 10-00 UT, d) 20 Sep 16-00 UT, e) 21 Sep 0-3 UT, f) 21 Sep 16-00UT, and g) 02 Oct 04-14 UT.**
54 **Pink dots are overlaid to indicate the simulated tropopause altitude based on a blended estimate (TROPPB).**

55
56
57



58
59
60
61
62
63
64
65
66



67
68

69 **Figure 3: Ozone number density values for the TROPOZ lidar, GEOS-CF mode, TROPOMI and electro-chemical cell**
70 **(ECC) ozonesondes at the 4km layers/levels.**

71
72
73
74
75
76

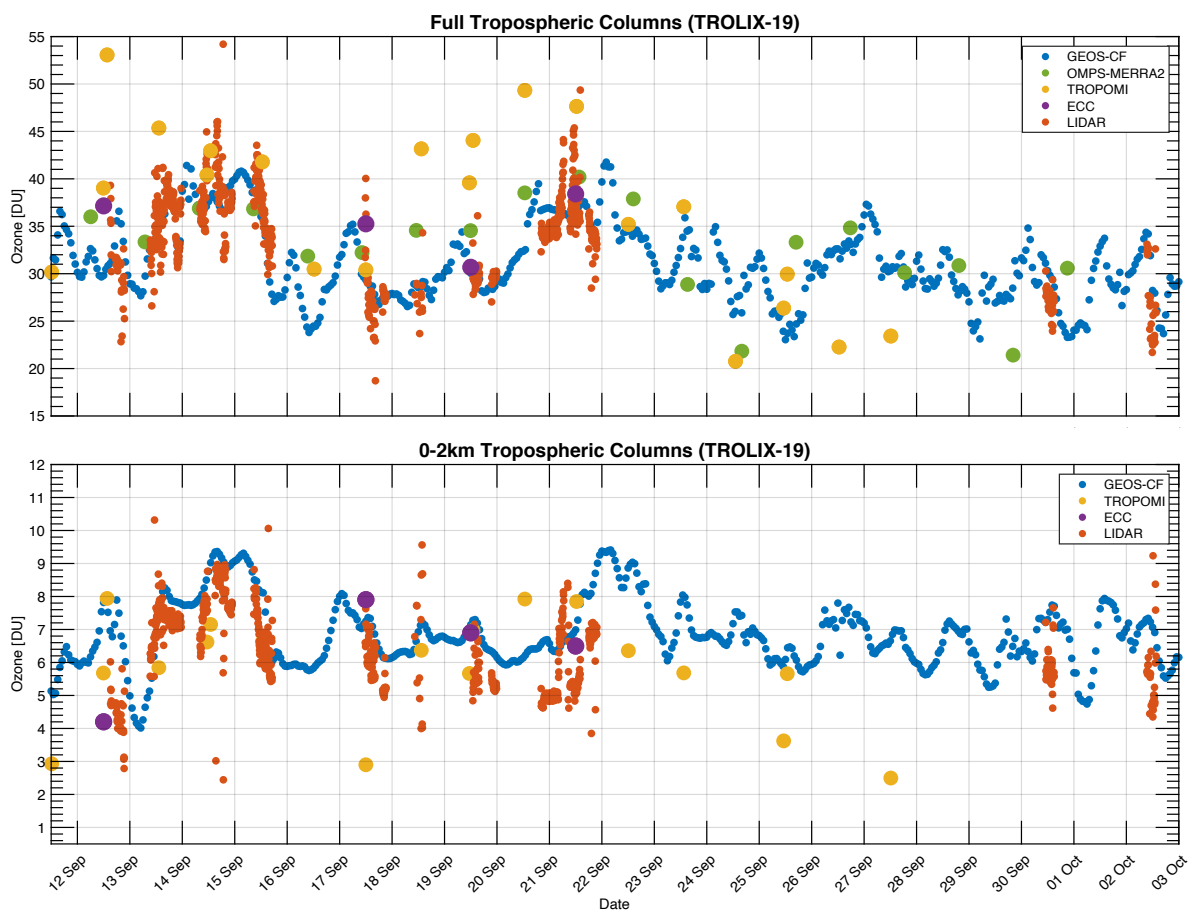


77

78

79

80



81

82 **Figure 4: Full tropospheric columns (top panel) and 0-2km tropospheric columns (bottom panel) calculated from**
83 **GEOS-CF, OMPS-MERRA2 (full column only), TROPOMI, Lidar and ECC.**

84

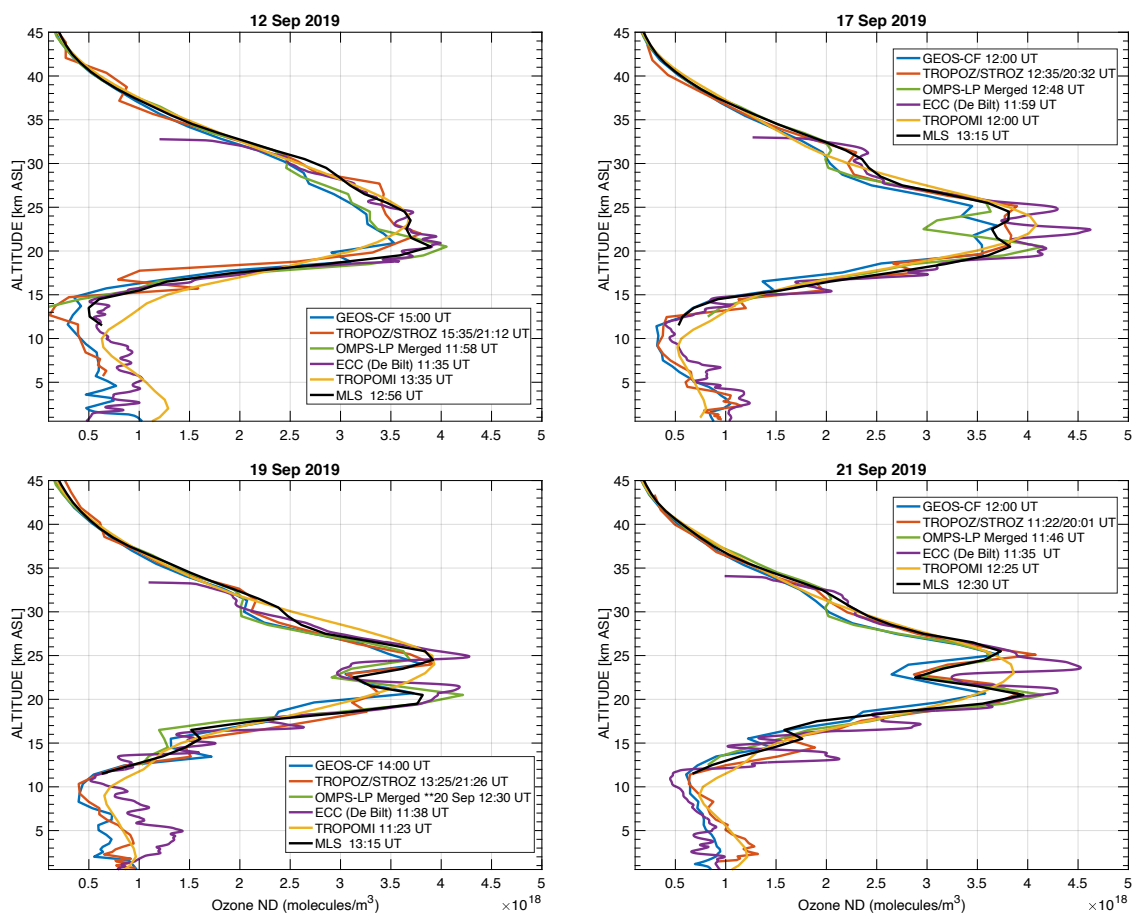
85

86

87



88
89
90



91
92

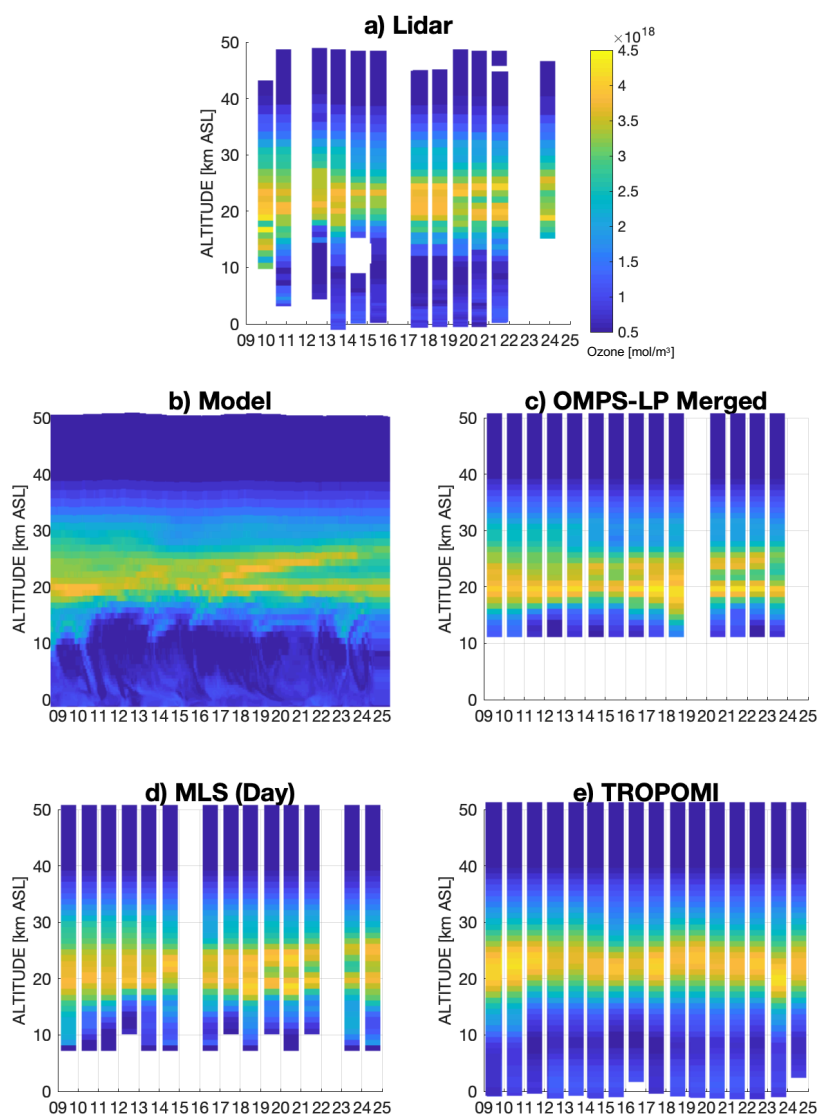
93 **Figure 5: GEOS-CF, Lidar, OMPS-LP, ECC, TROPOMI, and MLS ozone profile comparisons for 12 Sep, 17 Sep, 19**
94 **Sep, and 21 Sep 2019. These days were selected as days within the campaign that had an ECC launch from De Bilt.**

95
96
97



98

99



00

01 **Figure 6: Ozone number densities across all platforms for the TROLIX-19 time period from the hybrid lidar dataset**

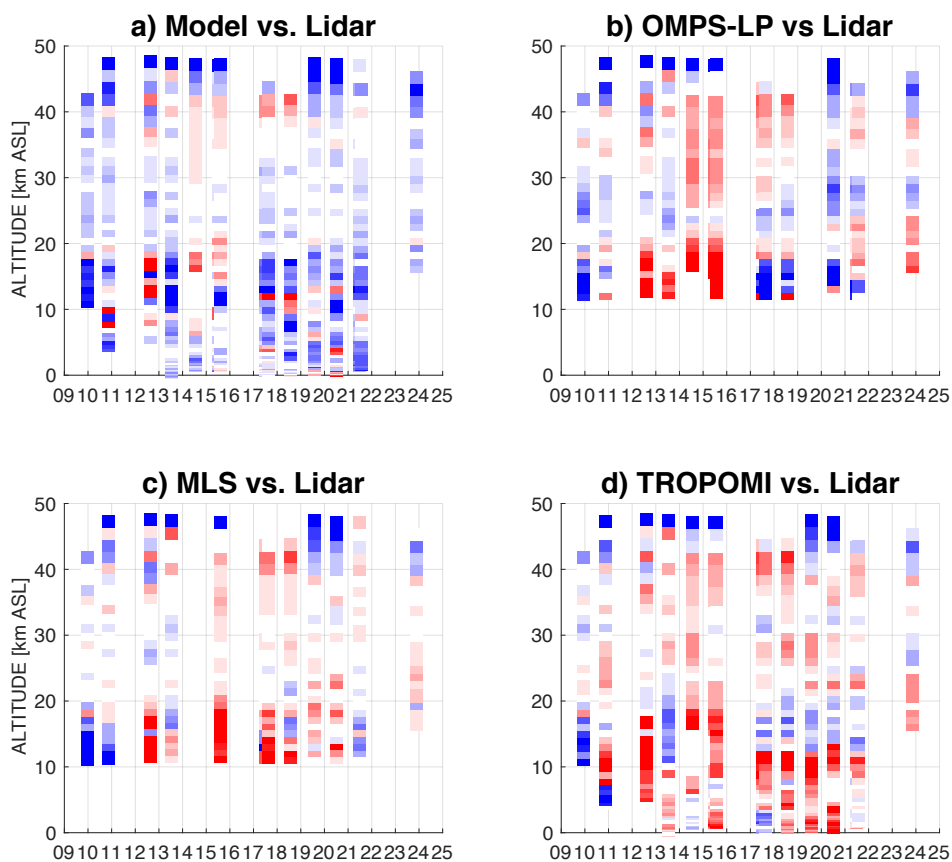
02 **(Figure 6a), GEOS-CF (Figure 6b), OMPS-LP (Figure 6c), MLS (Figure 6d), TROPOMI (Figure 6e). The x-axis as**

03 **day of September 2019.**

04



05
06
07
08



09

10 **Figure 7: Differences in ozone number densities across all platforms for the TROLIX-19 time period for Model (Figure**
11 **7a), OMPS-LP (Figure 7b), MLS (Figure 7c), and TROPOMI (Figure 7d). The x-axis as day of September 2019.**

12

13

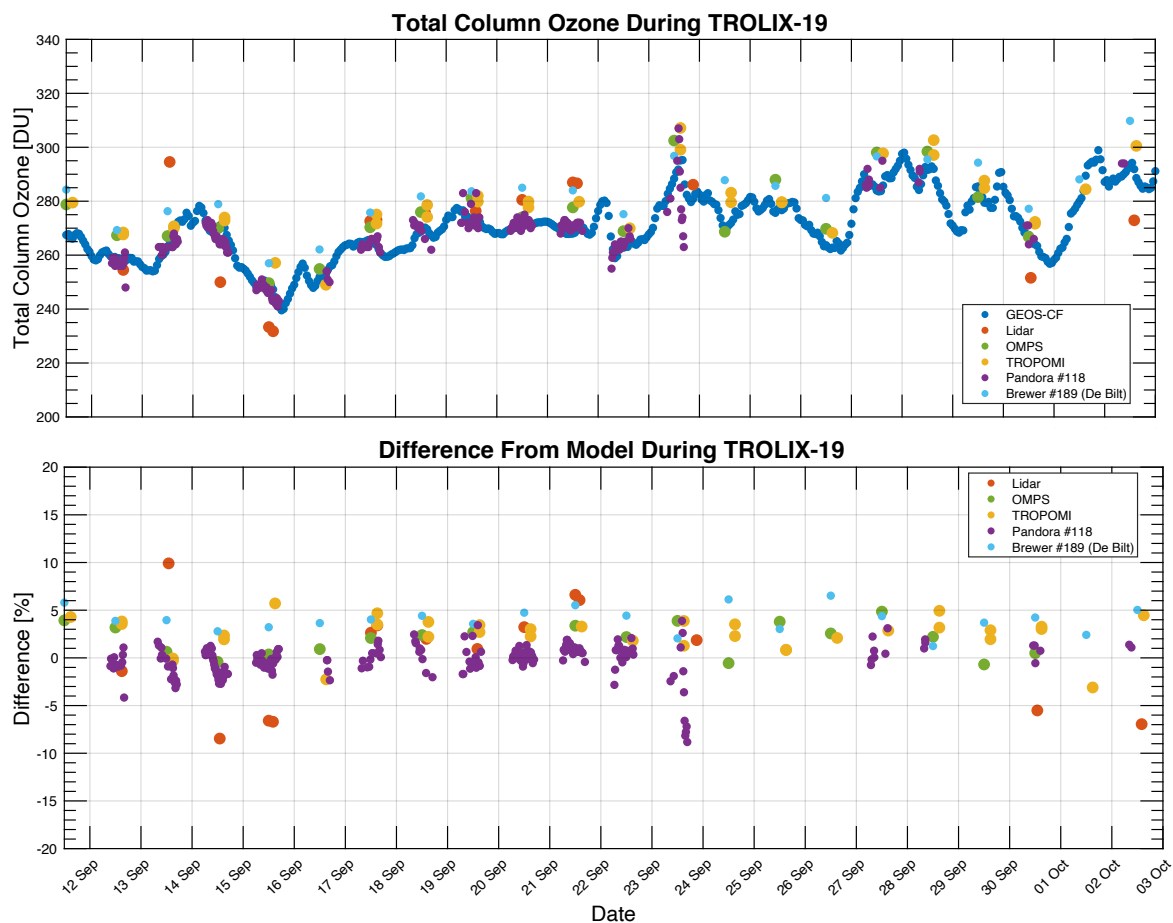
14

15

16



17



18

19 **Figure 8: Total Ozone columns (top panel) and percent differences (bottom panel) as compared to the model**
20 **observations for GEOS-CF, lidar, OMPS, TROPOMI, Pandora, and Brewer.**

21